Ballistic trajectories of optical wave packets within microcavities

Jean-Pierre Wolf*
LASIM (UMR CNRS 5579), Université Claude Bernard Lyon 1, 43, Boulevard du 11 Novembre 1918, 69622 Villeurbanne, France

Yong-Le Pan
Physical Sciences Laboratory, New Mexico State University, Las Cruces, New Mexico 88003

Gordon M. Turner, Matthew C. Beard, and Charles A. Schmuttenmaer
Department of Chemistry, Yale University, New Haven, Connecticut 06520-8107

Stephen Holler and Richard K. Chang
Department of Applied Physics, Yale University, New Haven, Connecticut 06520-8284
(Received 10 October 2000; published 10 July 2001)

We present time-resolved measurements of the ballistic trajectory of ultrashort optical wave packets circulating near the surface of a dielectric microcavity. The wave-packet dynamics are determined by using two-color two-photon induced fluorescence of Coumarin 510 within the microcavity as a correlator. Ballistic motion of the wave packets in whispering gallery modes and rainbow trajectories has been deduced from the time delay between collisions of the two wave packets. The cavity ringdown time is measured for each of the wave packets, which retain their integrity even after several round trips.

DOI: 10.1103/PhysRevA.64.023808 PACS number(s): 42.25.Bs, 33.80.Wz, 42.65.Re

Ballistic motion of a narrow optical wave packet within a wider resonator has been debated for more than 25 years [1,2]. In his pioneering work, Kastler [1] showed that a short pulse traveling within a Fabry-Perot resonator correctly reproduces the spectral transfer function of the interferometer, even though it does not overlap temporally with itself. The output intensity $I(t)$ is comprised of a train of pulses separated by the round-trip time. The intensity envelope decays with the average residence time τ of the photons in the cavity. The Fourier-transformed spectrum $I(\omega)$ reproduces the well-known Airy function, with associated resonance frequencies and finesse, or quality factor, of the Fabry-Perot interferometer [1].

This topic has recently been revisited in the context of cavity ring-down spectroscopy (CRDS), which is becoming widely used [3–6]. In CRDS, weak absorption spectra of gas molecules residing within a Fabry-Perot interferometer are determined by recording the ring-down time τ as a function of wavelength. CRDS has demonstrated much higher sensitivity (absorption coefficients as low as $10^{-8}\,\mathrm{cm}^{-1}$) than single path absorption techniques because of longer effective path length (as much as $30\,000\times$) and a relative insensitivity to exciting source fluctuations. However, controversy remained until recently regarding the correct description of excitation by pulses on the order of, or shorter than, the cavity length [4,6].

Recent experiments have been reported on the ballistic trajectories of THz wave packets scattered or reflected by a 6.35-mm dielectric sphere (alumina) [7]. The large sphere size used in those studies allowed the time of flight of the scattered wave packets to be measured directly. Extensive work has been dedicated to optical resonance in micrometer-sized objects, such as water droplets, glass spheres, and lithographically produced structures [8]. Nonlinear optical effects can be observed at low thresholds because of the strong optical fields at some resonator modes. Directional laser emission has even been demonstrated recently in stadium-shaped microcavities [9]. Microcavities usually support a wide variety of resonance modes, each with different associated quality factors Q. These modes consist of both chaotic orbits and stable orbits, such as triangles, squares, and bow-tie shaped, or whispering-gallery modes (WGM's). Light can also follow open, rainbow-type orbit trajectories inside the microcavity.

Until now, resonance modes have mainly been considered in the frequency domain by analyzing the spectra of fluorescence, elastically and Raman-scattered light, or laser emission having a pulse duration much longer than the round-trip time within the microcavities. Temporal behavior of the resonance modes on longer time scales, such as the temporal decay of high-Q WGM [10,11] and oscillation mode precession in nonspherical droplets [12], has been reported. Theoretical studies based on Lorenz-Mie theory have addressed the transient behavior of elastic scattering and the dynamics of mode buildup within spherical microcavities [13]. No direct time-resolved observation has been reported on the ballistic motion of localized wave packets within microcavities, however. In particular, several puzzling questions need to be answered: (i) Do the exciting wave packet remain intact after coupling into the cavity? (ii) After impact coupling, can the wave packets circulate in geometric orbits without being spread significantly by dispersion? (iii) Could an experimental scheme be found with sufficiently high time resolution to observe the wave packets' motion? A 100-fs pulse corresponds to a wave packet of light with a spatial length of about 30 μm in air, and about 20 μm in a dielectric with index of refraction $n=1.5$.

*Electronic address: wolf@lasim.univ-lyon1.fr

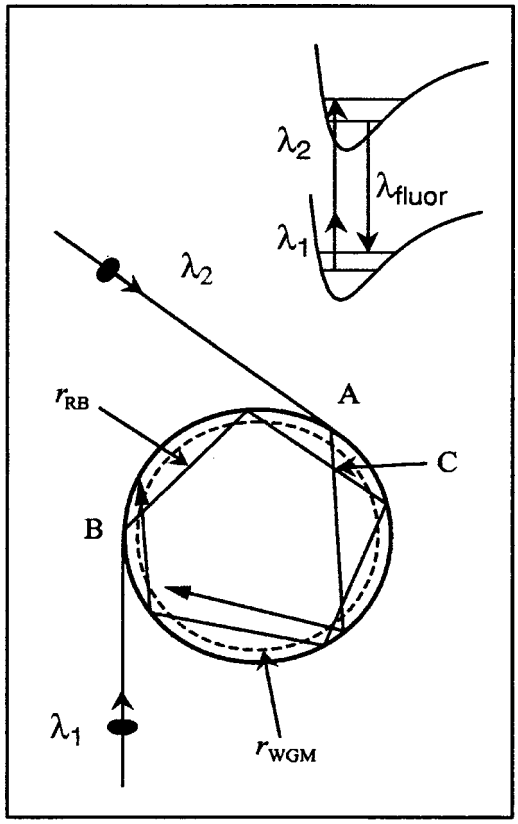

FIG. 1. Pulse correlator based on two-color two-photon excited fluorescence of Coumarin 510 dye molecules within a hanging pendent droplet. When coupled into a WGM, pulse λ_1 (1200 nm) meets pulse λ_2 (600 nm) at point *A*. Similarly, when pulse λ_2 is coupled into a WGM, it meets pulse λ_1 at point *B*. On the other hand, when both pulses travel along rainbow trajectories, they meet at *C*. The inset schematically displays the two-color two-photon excitation and fluorescence processes.

In this paper, we present time-resolved measurements of the ballistic motion of ultrashort optical wave packets ($\sim$100-fs pulse duration) within a spherical microcavity. We show, in particular, the coherent excitation of a large number of WGM's by using a 100-fs pulse, similar to mode locking in an ultrashort laser oscillator. After the wave packet has made one to two round trips around the sphere's equator, its temporal shape remains essentially unchanged, implying that coupling into multiple modes occurred without significant decoherence. This process can be compared to temporal coherent control of electronic or vibronic states in atoms [14] and molecules [15], creating localized wave packets that oscillate within potential wells. In recent experiments on Cs atoms, Girard *et al.* [16] compared the effects of quantum interferences among atomic states and interferences between optical wave packets in a pump-probe-type arrangement.

A novel experimental scheme has been developed (Fig. 1) to serve as an optical correlator between a wave packet at one wavelength ($\lambda_1 = 1200$ nm) with another wave packet at a different wavelength ($\lambda_2 = 600$ nm), which are both circulating on ballistic orbits. More specifically, we use two-color two-photon-excited fluorescence of Coumarin 510 dye molecules imbedded in the microcavity as the experimental observable for the spatial and temporal coincidence of both wave packets (see the inset of Fig. 1). The fluorescence intensity near 510 nm is then recorded as a function of the time delay between the two wave packets in order to quantify the path length traveled within the cavity. The micrometer-sized resonators investigated consist of hanging pendent ethylene glycol microdroplets (500–700 μm in radius), which have slow evaporation rate and, therefore, allowed for measurements over several minutes without significant change in size. Specifically, 2 g/L of C510 was first dissolved in ethanol, and then diluted 5:1 in ethylene glycol. A capillary tube (inner diameter 150 micrometer and outer diameter 250 micrometer) was then filled with the dye-containing solution. The capillary tube was held vertically, and equilibrium between surface tension and gravity led to a stable droplet. Any evaporation over the course of the experiment was compensated by additional liquid from the reservoir remaining in the capillary.

The femtosecond pulses were generated with an optical parametric oscillator and amplifier (OPA) by using 800-nm pulses from a regeneratively amplified Ti: sapphire laser. The regenerative amplifier has 1-kHz repetition rate, and produces pulses of 100-fs duration with roughly 900-μJ energy. After the OPA, the signal beam at 1200 nm has $\approx$70 μJ, and 20 μJ is obtained at 600 nm (after frequency doubling of the signal beam). Neutral density filters are introduced to reduce the energies used in the experiments: 1 μJ at $\lambda_1 = 1200$ nm and 0.2 μJ at $\lambda_2 = 600$ nm. The relative timing between the two pulses is achieved by an optical delay line that is controlled by a stepper motor fitted with a linear encoder to yield 1-μm absolute positional accuracy, which corresponds to 6.67 fs. The beams are focused to $\sim$60-μm-diam spot size for most efficient coupling into the microdroplet. The emitted fluorescence (two-color, two-photon induced fluorescence from the C510 dye in the droplet) was collected by a lens ($f = 5$ cm, the numerical aperature is 0.2), spectrally analyzed with a 1/10 m monochromator (Jobin Yvon H-10), and detected by a blue sensitive photomultiplier (Hamamatsu H6780-04) covered with a green narrow-bandpass filter.

Background emission in the correlator is generated from three-photon excited fluorescence (3PEF) from the infrared λ_1 pulse as well as from two-photon excited fluorescence (2PEF) from the λ_2 pulse. The three-photon excitation cross section is very small. Therefore, the primary source of noise is 2PEF, which was dramatically reduced by chopping beam λ_1 and using lock-in detection. The 3PEF and 2PEF are one-color processes that induce a constant offset in the time-delay profile, but are independent of the time delay between λ_1 and λ_2 wave packets.

Figure 2(a) displays the fluorescence intensity as a function of time delay between pulses λ_1 and λ_2. The beams were adjusted to be tangent to the surface of the droplet ($r = 700\,\mu$m, monitored by a CCD camera) in order to excite WGM's. Positive time delays refer to the λ_1 pulse reaching the droplet before the λ_2 pulse. Figure 2(a) clearly shows two peaks separated by the round-trip time. This result constitutes a time-resolved observation of the ballistic motion of optical wave packets within a microcavity. The first coincidence between the two wave packets occurs at location *A*

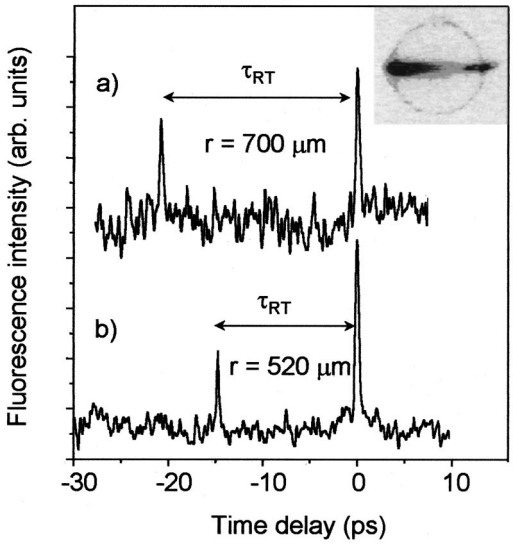

FIG. 2. Observation of the ballistic motion of femtosecond wave packets trapped in WGM's of pendent droplets of two different sizes. The measured round-trip time is denoted τ_{RT}. A CCD image of the droplet showing the fluorescence intensity distribution is displayed in the inset.

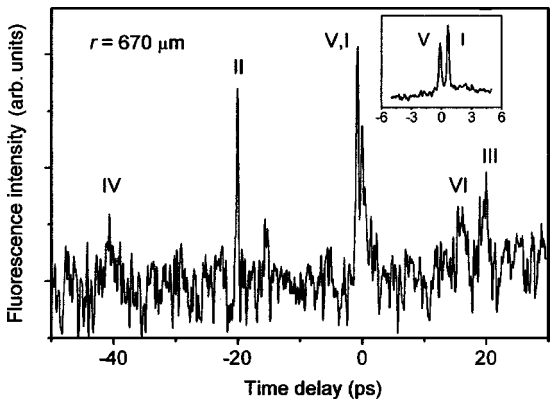

FIG. 3. Time-resolved measurement of the trajectories of both λ_1 and λ_2 wave packets on longer time scales. Positive times correspond to circulation of pulse λ_1, and negative times for the motion of pulse λ_2. Peaks I and V are due to the propagation of pulse λ_1 along a WGM and rainbow trajectory, respectively. The inset displays a higher time-resolution scan over the time zero region. It was taken with a slightly larger impact parameter, thereby enhancing the WGM peak. Peak II is due to the circulation of pulse λ_2. The decrease in fluorescence intensity of additional round-trip peaks (III and IV) can be used to deduce cavity lifetimes as in CRDS. Peak VI is due to a round-trip rainbow trajectory of pulse λ_1.

(see Fig. 1) and is chosen as time $t=0$. To reach location A and to meet the λ_2 pulse there, the λ_1 pulse must first travel around $\frac{3}{8}$ of the circumference. The other peak in Fig. 2(a) occurs when the pulses are coincident at location B, after the λ_2 pulse has traveled $\frac{5}{8}$ of the circumference. The expected round-trip time is given by $\tau_{RT}=2\pi rn/c$ (where r is the droplet radius, n is the refractive index$=1.43$, and c is the speed of light), and is in perfect agreement with the measured round-trip time of 21 ps.

Figure 2(b) shows the same type of time delay scan for a smaller size droplet ($r=520\,\mu$m), with a concomitant decrease in τ_{RT}. Because the temporal linewidth of correlation peaks ($\sim$250 fs) do not significantly exceed the correlation time of the two interacting 100-fs pulses, we conclude that the 100-fs wave packets survive evanescent coupling into WGM's without temporal spreading. In addition, the femtosecond pulses must coherently excite a large number of WGM's whose phases remain locked for at least a round-trip time.

Figure 3 shows that additional weaker peaks appear at longer time delays (a droplet with $r=670\,\mu$m is shown, but these results are generic). The peaks at $+20$ and -40 ps are due to an additional round trip of the λ_1 pulse and the λ_2 pulse, respectively. A slight difference is found (0.2 ps) between the round-trip times for each wavelength, consistent with the slightly differing indices of refraction at two wavelengths [$n(\lambda_2)=1.43$ and $n(\lambda_1)=1.42$]. However, the optical wave packets may travel on circular trajectories slightly smaller than the geometrical circumference of the droplet, depending on which radial order of the WGM modes is excited [17]. After the additional round trip, the temporal peak width increases to about 2 ps, indicating some relative phase spread among the numerous WGM's excited by the λ_1 and λ_2 pulses.

Furthermore, the additional peaks at $+20$ ps (peak III in Fig. 3) and at -40 ps (peak IV) allow the decay time τ of the photons in the cavity at both wavelengths to be estimated, which constitutes the first CRDS experiment within a microcavity. At 600 nm, $\tau\approx 18$ ps while at 1200 nm, $\tau>60$ ps. The average mode quality factor (defined as $Q=\omega_0\tau$) is thus $\approx 4\times 10^4$ at 600 nm and $\approx 7\times 10^4$ at 1200 nm. This relative low-Q value indicates that the average photon lifetime in the cavity is limited by both diffraction and residual multiphoton absorption. The 3PEF absorption cross section is indeed much smaller than 2PEF, which introduces lower absorption loss for λ_1.

In order to estimate the number of modes coherently coupled by the 100-fs pulse, we calculate the range of size parameters, Δx, encompassed within the laser bandwidth, $\Delta\lambda$ (15 nm), in the spectral domain. For $r=670\,\mu$m and $\lambda=1.2\,\mu$m, $\Delta x=(2\pi r/\lambda)(\Delta\lambda/\lambda)=44$, with a mean size parameter value of $x=3500$ ($x=2\pi r/\lambda$). The density of modes, ρ_{nl}, for a sphere illuminated by a plane wave without taking into account the degeneracy on the azimuthal mode number m, is $x/5$ in this size parameter range [18], i.e., $\rho_{nl}=700$. Thus, the number of modes excited within the size parameter range Δx would be 30 800. However, the excitation occurs on the rim with a beam waist $\sim$10 times smaller than the droplet radius, so we estimate that only 10% of them are excited, or about 3000. The m degeneracy ($2l+1$, where l is the angular momentum number) will increase the total number of modes by a factor 40 [19], even though it is also reduced by the rim excitation, leading finally to about 10^5 modes. This large number of modes allows a very well localized wave packet by coherent excitation, although probably 10–100 modes would be sufficient to do so. These considerations support the assertion that similar behaviors are

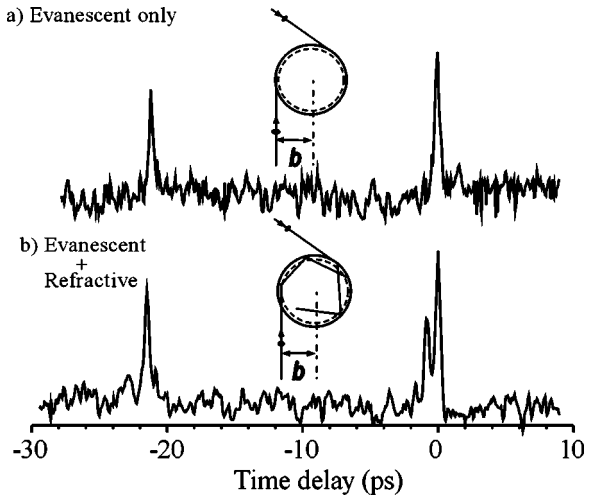

FIG. 4. Competition between WGM and rainbow-type orbits. Coupling of the external pump beam with the rainbow-type trajectories decreases upon moving the pump beam further from the droplet center. The impact parameter is denoted as *b*.

expected for much smaller size parameters, and thus smaller particles.

The wave-packet circulation in surface modes competes with ballistic motion in rainbow trajectories (see Fig. 1). Interpretation of the related peaks has been performed using a ray-tracing code. In particular, a doublet is found in this experiment near time zero, as shown in the inset of Fig. 3. The right-hand peak is identified as involving WGM orbits (see above), the left-hand peak corresponds to the coincidence at location *C* of λ_1 moving on a rainbow trajectory after one internal reflection and the λ_2 pulse that is refractively coupled into the droplet. The calculated difference in path lengths between the WGM and rainbow trajectories matches the observed 750-fs time difference of the doublet. Similarly, the peak at 16.20 ps (peak VI) corresponds to a round-trip time of the λ_1 pulse traveling along the internal rainbow mode after four reflections, before meeting the incoming λ_2 pulse at *A*.

The relative coupling of the external wave with WGM's (via evanescent wave) and the rainbow trajectories (via refraction) has been further investigated by varying the impact parameter of beam λ_1 while keeping the position of the λ_2 beam fixed (Fig. 4). These measurements confirm unambiguously the association of each peak of the doublet structure with a particular trajectory of the pump beam. The effect of the impact parameter *b* of a Gaussian beam onto the droplet is well known: the beam excites WGM's when it is tangent to the surface, and it follows rainbow trajectories when it is moved further towards the center [20]. Accordingly, the left peak of the doublet in Fig. 4(b) at $t=0$ vanishes when the pump beam is moved away from the droplet center, causing the refractive coupling to be reduced, and resulting in a single peak [Fig. 4(a)].

In summary, these time-resolved measurements with femtosecond pulses demonstrate that the optical wave packet is preserved as it couples into and circulates within WGM's around the equator of a hanging pendent droplet. These observations open new perspectives for studying ballistic trajectories and absorptions in microcavities, such as trace detection in microdroplets, *Q* control in microresonators, and mode characterization in deformed resonators.

R.K.C. and S.H. acknowledge financial support from the Air Force Office of Scientific Research (Contract No. F49620-00-1-0182). C.A.S. and R.K.C. acknowledge the NSF (Grant No. CHE-9601824) for partial funding toward the purchase of the ultrafast laser/OPA system. Y.L.P. acknowledges financial support from the U.S. Army Research Laboratory (ARL Contract No. DAAL01-98-C0056). J.P.W. acknowledges NATO's support. The authors gratefully thank Dr. Steven C. Hill at ARL for very helpful discussions.

[1] A. Kastler, Nouv. Rev. Opt. **5**, 133 (1974).
[2] C. Roychoudhuri, J. Opt. Soc. Am. **65**, 1418 (1975).
[3] P. Zalicki and R. N. Zare, J. Chem. Phys. **102**, 2708 (1995).
[4] K. K. Lehmann and D. Romanini, J. Chem. Phys. **105**, 10 263 (1996).
[5] A. O'Keefe, J. J. Scherer, A. L. Cooksy, R. Sheeks, J. R. Heath, and R. J. Saykally, Chem. Phys. Lett. **172**, 214 (1990).
[6] J. J. Scherer, J. B. Paul, A. O'Keefe, and R. J. Saykally, Chem. Rev. **97**, 25 (1997).
[7] R. A. Cheville, R. W. Mc Gowan, and D. Grischkowsky, Phys. Rev. Lett. **80**, 269 (1998).
[8] P. W. Barber and R. K. Chang, *Optical Effects Associated with Small Particles* (World Scientific, Singapore, 1988).
[9] C. Gmachi, F. Capasso, E. E. Narimanov, J. U. Noeckel, A. D. Stone, J. Faist, D. L. Sivco, and A. Y. Cho, Science **280**, 1556 (1998).
[10] V. Sandoghdar, F. Treussart, J. Hare, V. Lefevre-Seguin, J. M. Raimond, and S. Haroche, Phys. Rev. A **54**, R1777 (1996).
[11] D. S. Weiss, V. Sandoghdar, J. Hare, V. Lefevre-Seguin, J. M. Raymond, and S. Haroche, Opt. Lett. **20**, 1835 (1995).
[12] J. C. Swindal, D. H. Leach, R. K. Chang, and K. Young, Opt. Lett. **18**, 191 (1993).
[13] D. Q. Chowdhurry, P. W. Barber, and S. C. Hill, J. Opt. Soc. Am. A **9**, 1364 (1992).
[14] J. Bromage and C. R. Stroud, Jr., Phys. Rev. Lett. **83**, 4963 (1999).
[15] T. Baumert, M. Grosser, R. Thalweiser, and G. Gerber, Phys. Rev. Lett. **67**, 3753 (1991).
[16] V. Blanchet, C. Nicole, M. A. Bouchene, and B. Girard, Phys. Rev. Lett. **78**, 2716 (1997).
[17] S. C. Hill and R. E. Benner, in *Optical Effects Associated with Small Particles*, edited by P. W. Barber and R. K. Chang

(World Scientific, Singapore, 1988).

[18] Steve Hill (private communication).

[19] It is known that $m/l=\cos(\theta_m)$ [12]. The angle subtended by the laser beam waist in this work is only $\theta=\tan^{-1}(w/r)=6°$, where w is the beam waist size and r is the droplet radius. Therefore, the excited m states can only have values corresponding to θ_m between 0° and 6°. Thus, $0.995*l<|m|<l$ and the total number of m values for a given l is roughly 1% of l. Since l lies between x and nx for WGM's, we find about 40 m modes for each l value (1% of $x\sim4000$).

[20] See, for example, E. E. M. Khaled, S. C. Hill, and P. W. Barber, IEEE Trans. Antennas Propag. **41**, 295 (1993); J. P. Barton, W. Ma, S. A. Schaub, and D. R. Alexander, Appl. Opt. **30**, 4706 (1991).